JOURNAL OF APPLIED PHYSICS **114**, 174108 (2013)

Shell model of $BaTiO_3$ derived from *ab-initio* total energy calculations

J. M. Vielma and G. Schneider[a)]
Department of Physics, Oregon State University, Corvallis, Oregon 97331, USA

(Received 6 September 2013; accepted 14 October 2013; published online 7 November 2013)

A shell model for ferroelectric perovskites fitted to results of first-principles density functional theory (DFT) calculations is strongly affected by approximations made in the exchange-correlation functional within DFT, and in general not as accurate as a shell model derived from experimental data. We have developed an isotropic shell model for $BaTiO_3$ based on the PBEsol exchange-correlation functional [Perdew *et al.*, Phys. Rev. Lett. **100**, 136406 (2008)], which was specifically designed for crystal properties of solids. Our shell model for $BaTiO_3$ agrees with ground state DFT properties and the experimental lattice constants at finite temperatures. The sequence of phases of $BaTiO_3$ (rhombohedral, orthorhombic, tetragonal, cubic) is correctly reproduced but the temperature scale of the phase transitions is compressed. The temperature scale can be improved by scaling of the *ab-initio* energy surface. © *2013 AIP Publishing LLC*. [http://dx.doi.org/10.1063/1.4827475]

I. INTRODUCTION

Ferroelectric perovskites or perovskite solid solutions near a ferroelectric instability have potential applications as fast capacitive storage medium[2,3] and considerable interest exists to develop lead-free ferroelectric materials to replace the widely used piezoelectric $Pb(Zr,Ti)O_3$ (PZT).[4,5] Systematic selection and improvement of materials and properties for applications depends on the detailed knowledge of the physics in these materials, which frequently requires understanding of phenomena over medium and long length and time scales. Atomistic model simulations of ferroelectric perovskites, such as isotropic[6] and anisotropic[7] shell models (SMs) and approaches based on effective Hamiltonians,[8] can probe length and time scales that are beyond the reach of computationally much more demanding first-principles simulations. In order to observe finite temperature phase transitions, broad stoichiometric ordering of solid solutions and nano-scale properties within a bulk material or thin films (e.g., grain boundaries, domain walls), simulation cells must contain thousands of atoms. Both the shell model and the effective Hamiltonian have free parameters that are fitted from experimental and first-principles observations. Fitting an isotropic shell model to first principles density functional theory (DFT) calculations is generally easier than an effective model Hamiltonian, which is much more complex. In addition, a shell model retains information on atomic positions.

The accuracy of a shell model depends on both the complexity of the model and on the accuracy of the data used to fit the model, which for DFT depends on approximations made in the exchange-correlation functional. Isotropic shell models fitted to results from DFT calculations have successfully described the qualitative behavior of ferroelectric perovskites.[6,9–13] A shell model of $BaTiO_3$, fitted to DFT using the local density approximation (LDA), significantly underestimates the lattice constants, polarizations, and phase transition temperatures of $BaTiO_3$.[9] Scaling of the lattice constant to the experimental values does not correct issues with the magnitude of polarization and phase transition temperatures,[7] and introduces inconsistencies across different supercell sizes. The generalized gradient approximation (GGA) within DFT as implemented by Perdew, Burke, and Ernzerhoff (PBE)[14] improves the accuracy of the lattice constants of all phases and energy differences between phases, but it severely overestimates the tetragonal strain and volume of each unit cell.[12,15] The failure of the mentioned approximations is due to the sensitivity of perovskite ferroelectric properties to pressure. Increasing the pressure significantly decreases the well depths in the potential energy surface.[16]

To improve on the issues with LDA and GGA/PBE in DFT calculations of perovskites, two other forms for the exchange-correlation functional have been considered: the weighted density approximation (WDA)[17–20] and the Perdew-Burke-Ernzerhof generalized gradient approximation for solids (PBEsol).[1] WDA gives much better cubic lattice constants for $BaTiO_3$, but it does not improve the volume and strain of the other phases compared to LDA and PBE.[15] The modification of PBE for solids (PBEsol) leads to very accurate lattice parameters for the ground state;[21] it slightly underestimates the cubic lattice constant and cuts the percentage error to one-third relative to LDA and PBE. PBEsol does overestimate the *c*/*a* ratio of the tetragonal phase but less than PBE.[22] PBEsol also gives much better oxygen-titanium displacements in $BaTiO_3$.

In this paper, we will discuss an isotropic shell model for $BaTiO_3$ fitted to results from DFT calculations using PBEsol. $BaTiO_3$ is chosen, since it has a rich phase diagram and it has been used frequently for shell models, which allows for comparisons.[7,10,11,23–25] In Sec. II, the shell model is discussed as well as the methods behind the fitting procedure and DFT calculations. In Sec. III, the result of our model are presented and compared to both the results of *ab initio* DFT calculations and experimental data for bulk properties at finite temperatures. Our conclusions are given in Sec. IV.

II. THEORY AND METHODS

The isotropic shell model treats an atom as two coupled charged particles connected by a spring: a core, which holds

[a)]Electronic mail: Guenter.Schneider@physics.oregonstate.edu

the atomic mass of the atom, and a massless shell. All cores and shells interact by Coulomb's law except the core and shell of the same atom. A short-range interaction that interacts only between shells of different atoms describes both electron cloud repulsion and van der Waals attraction. The short-range interaction chosen is the Buckingham potential and has the form $V(r) = A\exp(-r/\rho) - C/r^6$. The coupled core and shell interact via an anharmonic spring $V(r) = k_2 r^2/2 + k_4 r^4/24$. Hence, the free parameters in the shell model consist of the core and shell charges and the constants in the Buckingham and anharmonic spring potentials. Overall, charge neutrality adds one constraint for the charges.

The free parameters for the shell model are found through least squares minimization of the energy differences in the potential energy surface between the SM and the DFT calculations (Eq. (1)). The perfect cubic structure was chosen as the reference structure. Minimization of Eq. (1) was achieved using the Nelder-Mead Downhill Simplex Method[26]

$$\chi^2 = \sum_{i=1}^{N} \sigma_i^2 [(E_{C,DFT} - E_{i,DFT}) - (E_{C,SM} - E_{i,SM})]^2. \quad (1)$$

2200 configurations of the cubic, tetragonal, orthorhombic, and rhombohedral phases of $BaTiO_3$ were used for the fitting. Configurations include randomly displaced atoms from their optimal positions as well as changes in volume and strain. To determine the shell model energy E_{SM}, for each configuration using a trial set of the shell model parameters, the core of each atom is placed at the ionic position of the atom in the DFT configuration. The shell model energy E_{SM} is determined by relaxing the shells. Configurations with energies lower than the cubic phase and with energies close to any of the four phases of $BaTiO_3$ are emphasized using a weight factor, σ_i, to reproduce the DFT lattice constants accurately.

DFT calculations using the PBEsol exchange correlation functional were performed using the projector augmented plane wave (PAW) method as implemented in the Vienna *ab-initio* simulation package (VASP).[27,28] The plane-wave cutoff was set to 600 eV and Brillouin-zone integration was performed using a $6 \times 6 \times 6$ Monkhorst-Pack (MP) k-point mesh,[29] using the tetrahedron method.[30] For each configuration, the constrained ground state was found by relaxing the geometry until the maximum force on all atoms was less than 0.01 eV/Å. The orthorhombic and tetragonal states were found by relaxing the geometry of the unit cell while restricting the movement of the titanium atom relative to the barium atom to the [110] and [001] directions, respectively. Convergence was tested by comparing the calculated zero temperature lattice constants and energies of all four phases of $BaTiO_3$ with calculations using a plane-wave cutoff of 800 eV and a $8 \times 8 \times 8$ MP k-point mesh. Lattice constants and total energies were converged to better than 0.002 Å and 1 meV/atom, respectively. Our calculated unit cell parameters agree very well with previously reported values.[21,22]

TABLE I. Shell model parameters[a] based on DFT total energies using the PBEsol exchange correlation functional and determined by least square minimization (see text).

Atom	Core charge	Shell charge	k_2	k_4
Ba	4.859	−2.948	311.64	0.0
Ti	4.555	−1.615	332.55	500.0
O	1.058	−2.675	46.31	6599.24
Short-range	A	ρ	C	
Ba-O	1588.36	0.3553	0.0	
Ti-O	3131.25	0.2591	0.0	
O-O	2641.41	0.3507	535.37	

[a]Core and shell charges are in units of electrons, energies in units of eV, and lengths in units of Å.

III. RESULTS AND DISCUSSION

The shell model parameters derived for $BaTiO_3$ from the fit of PBEsol total energies are listed in Table I. Table I lists 21 parameters, of which 16 were determined in the fitting procedure. Effectively, one core charge is determined from charge neutrality. The repulsive k_4 parameters in the Buckingham potential for the cations were adapted from the work by Sepliarsky *et al.*[11] They help in the fitting procedure, in particular, by constraining the Ti shell, but they have a negligible effect on the shell model energies. The van der Waals interaction from the cations to the oxygen atoms was set to zero because the separation between the core and the shell of the cations is so small that they also have negligible effect on the shell model energies. Table II summarizes the zero temperature properties for all four phases of $BaTiO_3$ using the parameters from Table I. All lattice parameters for the shell model are within 0.01 Å of the DFT lattice parameters. The energy differences between the phases are overestimated by the shell model by ~2 eV or 10% relative to the DFT energy differences (Table II). Using the shell model the finite temperature behavior of $BaTiO_3$ can be determined form molecular dynamic (MD) simulations. All MD simulations were carried out using DL-POLY in a $10 \times 10 \times 10$ supercell with periodic boundary conditions and variable cell shape in a (N, σ, T) ensemble at atmospheric pressure.[31] The barostat and thermostat relaxation times are set to 0.1 ps each. All shells are assigned a mass of 2 a.u., so that the shell motion can be treated dynamically.[12] The time step used is

TABLE II. SM and scaled SM 0 K properties of all four phase of $BaTiO_3$ and comparison to DFT results. ΔE is the energy of a phase relative to the cubic phase (see text).

Phase		DFT (PBEsol)	SM	Scaled SM
Cubic	a_o (Å)	3.985	3.985	3.983
	ΔE (meV)	18.8	20.7	44.9
Tetra	a (Å)	3.971	3.975	3.968
	c/a	1.023	1.022	1.028
	ΔE (meV)	24.0	25.7	56.8
Orth	a (Å)	3.964	3.971	3.961
	$c/a, b/a$	1.015	1.014	1.018
Rhom	ΔE (meV)	25.3	27.8	59.4
	a (Å)	4.005	4.008	4.010

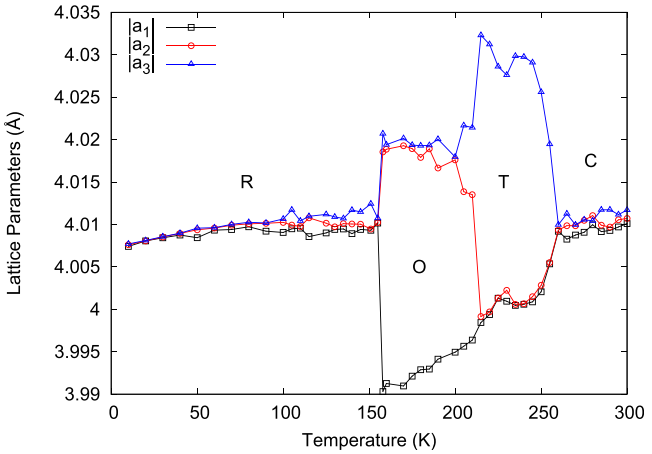

FIG. 1. Average lattice constants for all three lattice vectors for the $BaTiO_3$ phases (cubic (C), tetragonal (T), orthorhombic (O), rhombohedral (R)) as a function of temperature determined from MD simulations using the shell model (see text).

0.4 fs, the system is equilibrated for 4 ps, followed by a simulation run for 12 ps. The temperature dependent results of the MD simulations are shown in Figures 1 and 2. The shell model does reproduce the correct sequence of phase transitions: Rhombohedral (0–150 K) → Orthorhombic (150–210 K) → Tetragonal (210–260 K) → Cubic. The experimental phase transitions occur at 183, 278, and 393 K. The PBEsol based shell model consistently underestimates the temperatures of the phase transition temperatures, similar to the previous work using shell models fitted from DFT using LDA,[9] and from DFT using LDA with scaled lattice constants.[7] Averaged finite temperature lattice constants extracted from the MD simulations are summarized in Table III and with a maximum difference of 0.01 Å, agree very well with experimental values. The tetragonal and orthorhombic strains are slightly underestimated. The calculated absolute polarizations for the rhombohedral, orthorhombic, and tetragonal phases are 0.225, 0.198, and 0.15 C m^{-2}, respectively. These values underestimate the experimental values, 0.33, 0.36, and 0.27 C m^{-2}, by 55%–68%. This large disagreement is a result of emphasizing energy differences between configurations in the determination of the model parameters, while the polarization was not part of the fitness function. In the shell model, both the polarization and the total energy are very sensitive to the spring interaction between the oxygen core and the shell.[23] The phase transition temperatures can be improved by scaling the differences in the potential energy surface in the DFT calculations, which was successfully demonstrated using a shell model based on LDA total energies and extrapolated lattice constants.[10] Rescaling the potential energy differences in order to reproduce the rhombohedral-orthorhombic phase transition temperature results in the shell model parameters listed in Table IV. The MD simulation results for the scaled shell model are presented in Figures 3 and 4. The calculated phase

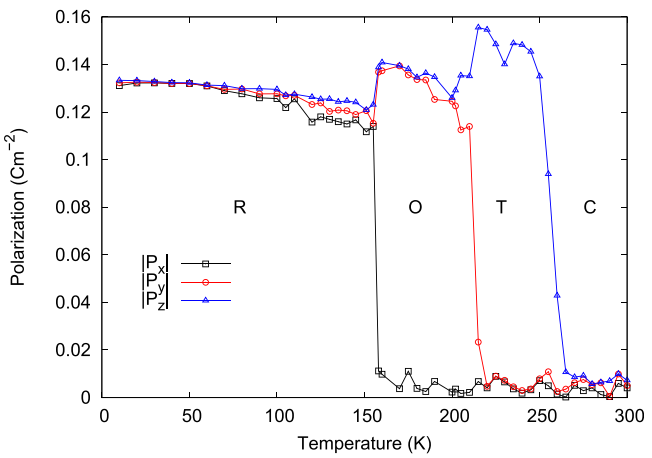

FIG. 2. Average absolute polarization in all three cartesian coordinates for the $BaTiO_3$ phases (cubic (C), tetragonal (T), orthorhombic (O), rhombohedral (R)) as a function of temperature determined from MD simulations using the shell model (see text).

TABLE III. Finite temperature shell model lattice constants extracted from MD simulations for all four phase of $BaTiO_3$ compared to experimental values.

Phase		Shell model	Scaled SM	Exp.
Cubic	a (Å)	4.01	4.01	4.00
Tetragonal	a (Å)	4.00	4.00	3.995
	c/a	1.008	1.011	1.010
Orthorhombic	a (Å)	4.00	3.99	3.985
	$c/a, b/a$	1.006	1.010	1.008
Rhombohedral	a (Å)	4.01	4.01	4.004

TABLE IV. Shell model parameters[a] based on the scaled DFT total energies using the PBEsol exchange correlation functional and determined by least square minimization (see text).

Atom	Core charge	Shell charge	k_2	k_4
Ba	5.042	−2.870	298.51	0.0
Ti	4.616	−1.544	306.14	500.0
O	0.970	−2.718	36.93	5000.0
Short-range	A	ρ	C	
Ba-O	7149.81	0.3019	0.0	
Ti-O	7200.27	0.2303	0.0	
O-O	3719.60	0.3408	597.17	

[a]Core and shell charges are in units of electrons, energies in units of eV, and lengths in units of Å.

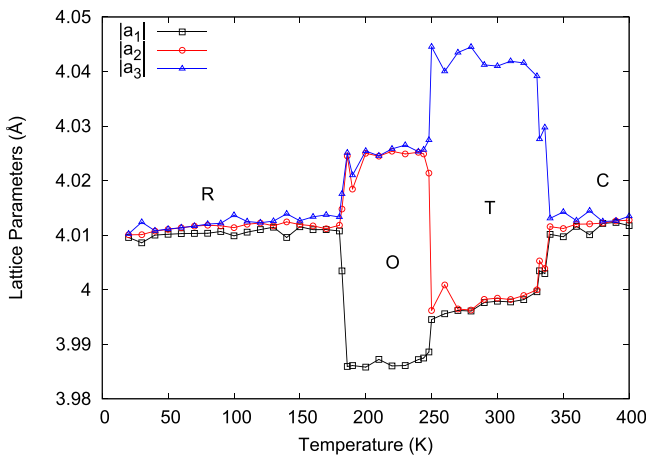

FIG. 3. Average lattice constants for all the three lattice vectors for $BaTiO_3$ as a function of temperature determined from MD simulations using the shell model fitted to scaled energy differences (see text).

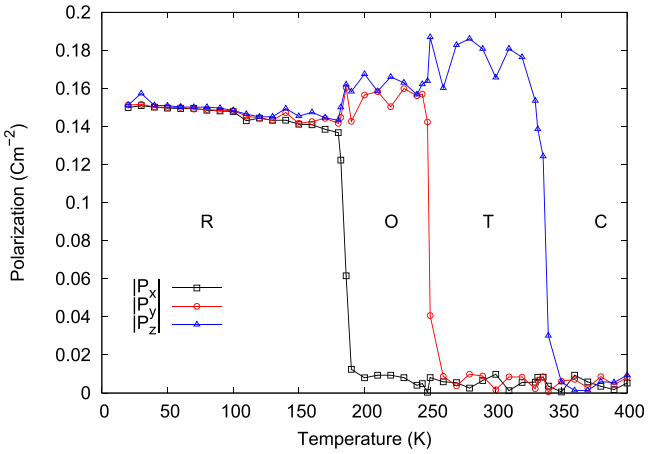

FIG. 4. Average absolute polarization in all three cartesian coordinates for $BaTiO_3$ as a function of temperature determined from MD simulations using the shell model fitted to scaled energy differences (see text).

transition temperatures using the scaled shell model are now 180 K, 250 K, and 340 K, respectively, in much better agreement with experimental values. At the same time, the lattice parameters of all 4 phases are practically unchanged when compared to the values obtained with the original, un-scaled shell model (Tables III and II). The calculated polarizations using the scaled shell model have increased slightly relative to the first shell model for all 3 non-cubic phases, but the values are still much small when compared to experimental values.

IV. SUMMARY AND CONCLUSIONS

We have developed and implemented an isotropic shell model from fitting total energy differences in the potential energy surface calculated using DFT with the PBEsol exchange correlation functional. Our model produces very accurate lattice constants when compared to the experimental lattice constants at finite temperatures. The sequence of phases of $BaTiO_3$ is reproduced correctly but the transition temperatures are too small. A scaling of the potential energy surface results in much better agreement for the phase transition temperatures, without sacrificing the accuracy of the lattice constants. Using total energies based on the PBEsol exchange correlation functional offers significant benefits over LDA or GGA based energies even for the basic isotropic shell model employed in this work. Various enhancements provide room for further improvement, such as an improved scaling of the energy differences, including *ab-initio* values of the polarization in the cost function, introducing a distance dependent spring constant $k_2(r)$ for the oxygen atoms,[23] and using an anisotropic spring constant for the oxygen core-shell system. Ultimately, the PBEsol functional holds significant promise for the successful development of shell models for more complex perovskite solid solutions entirely from *ab-initio* total energy calculations.

[1]J. P. Perdew, A. Ruzsinszky, G. I. Csonka, O. A. Vydrov, G. E. Scuseria, L. A. Constantin, X. Zhou, and K. Burke, Phys. Rev. Lett. **100**, 136406 (2008).
[2]C.-C. Huang and D. P. Cann, J. Appl. Phys. **104**, 024117 (2008).
[3]H. Ogihara, C. A. Randall, and S. Trolier-McKinstry, J. Am. Ceram. Soc. **92**, 110 (2009).
[4]S.-T. Zhang, A. B. Kounga, E. Aulbach, T. Granzow, W. Jo, H.-J. Kleebe, and J. Rodel, J. Appl. Phys. **103**, 034107 (2008).
[5]D. Y. Wang, N. Y. Chan, S. Li, S. H. Choy, H. Y. Tian, and H. L. W. Chan, Appl. Phys. Lett. **97**, 212901 (2010).
[6]M. Sepliarsky, S. R. Phillpot, D. Wolf, M. G. Stachiotti, and R. L. Migoni, Appl. Phys. Lett. **76**, 3986 (2000).
[7]S. Tinte, M. G. Stachiotti, M. Sepliarsky, R. L. Migoni, and C. O. Rodriguez, J. Phys: Condens. Matter **11**, 9679 (1999).
[8]K. M. Rabe and U. V. Waghmare, Ferroelectrics **136**, 147 (1992).
[9]M. Sepliarsky, Z. Wu, A. Asthagiri, and R. E. Cohen, Ferroelectrics **301**, 55 (2004).
[10]S. Tinte, M. G. Stachiotti, S. R. Phillpot, M. Sepliarsky, D. Wolf, and R. L. Migoni, J. Phys: Condens. Matter **16**, 3495 (2004).
[11]M. Sepliarsky, A. Asthagiri, S. Phillpot, M. Stachiotti, and R. Migoni, Curr. Opin. Solid State Mater. Sci. **9**, 107 (2005).
[12]A. Asthagiri, Z. Wu, N. Choudhury, and R. E. Cohen, Ferroelectrics **333**, 69 (2006).
[13]R. Machado, M. Sepliarsky, and M. G. Stachiotti, J. Mater. Sci. **45**, 4912 (2010).
[14]J. P. Perdew, K. Burke, and M. Ernzerhof, Phys. Rev. Lett. **77**, 3865 (1996).
[15]Z. Wu, R. E. Cohen, and D. J. Singh, Phys. Rev. B **70**, 104112 (2004).
[16]R. E. Cohen, Nature **358**, 136 (1992).
[17]O. Gunnarsson, M. Jonson, and B. I. Lundqvist, Phys. Rev. B **20**, 3136 (1979).
[18]O. Gunnarsson, M. Jonson, and B. I. Lundqvist, Phys. Lett. A **59**, 177 (1976).
[19]O. Gunnarsson, M. Jonson, and B. I. Lundqvist, Solid State Commun. **24**, 765 (1977).
[20]J. A. Alonso and L. A. Girifalco, Phys. Rev. B **17**, 3735 (1978).
[21]Z. Wu and R. E. Cohen, Phys. Rev. B **73**, 235116 (2006).
[22]R. Wahl, D. Vogtenhuber, and G. Kresse, Phys. Rev. B **78**, 104116 (2008).
[23]Y. Chen, B. Liu, Y. Ma, and Y. Zhou, Nucl. Instrum. Methods Phys. Res. B **267**, 3090 (2009).
[24]M. Sepliarsky and S. Tinte, Physica B **404**, 2730 (2009).
[25]X. Hu, G. Xie, and Y. Ma, Physica B **405**, 2577 (2010).
[26]W. H. Press, S. A. Teukolsky, W. T. Vetterling, and B. P. Flannery, *Numerical Recipes: The Art of Scientific Computing*, 3rd ed. (Cambridge University Press, New York, 2007).
[27]P. E. Blöchl, Phys. Rev. B **50**, 17953 (1994).
[28]G. Kresse and D. Joubert, Phys. Rev. B **59**, 1758 (1999).
[29]H. J. Monkhorst and J. D. Pack, Phys. Rev. B **13**, 5188 (1976).
[30]P. E. Blöchl, O. Jepsen, and O. K. Andersen, Phys. Rev. B **49**, 16223 (1994).
[31]W. Smith and T. R. Forester, "DL Poly," J. Mol. Graphics **14**, 136 (1996).